

A new species of the genus *Plagiostomum* (Platyhelminthes, Prolecithophora, Plagiostomidae), with description of its reproductive and developmental characteristics

Si-Qi Wang¹, Yong-Jian Ma¹, Hai-Long Liu^{1,2}, Ting Sun¹, An-Tai Wang¹, Yu Zhang^{1,3}

¹ Shenzhen Key Laboratory of Marine Bioresource and Eco-environmental Science, College of Life Science and Oceanography, Shenzhen University, Guangdong, China

² Key Laboratory of Optoelectronic Devices and Systems of Ministry of Education and Guangdong Province, College of Physics and Optoelectronic Engineering, Shenzhen University, Shenzhen, China

³ Guangdong Engineering Research Center for Marine Algal Biotechnology, College of Life Sciences and Oceanography, Shenzhen University, Shenzhen, Guangdong, China

<https://zoobank.org/C790F7A9-AC10-4783-BB32-D4513EACDAE2>

Corresponding author: Yu Zhang (biozy@szu.edu.cn)

Academic editor: Tom Artois ♦ Received 26 February 2025 ♦ Accepted 22 July 2025 ♦ Published 22 August 2025

Abstract

A new species of marine flatworm of the genus *Plagiostomum* is described from the intertidal zone along the coast of South China, based on comprehensive morphology, histology, reproductive biology, and molecular phylogenetic analyses. *Plagiostomum aestuarium* has a blunt anterior end with a small tentacle-like structure and a dark-brown patch covering the brain region. A pair of testes and a pair of ovaries are separated. The testes are located ventrally, while the ovaries are distributed from the vitellaria towards the testes. The vitellaria are separated at the anterior end, merge at the dorsal part of the intestine, and separate again at the posterior end on both sides of the intestine. The penis is encased in a well-developed penis sheath. The proximal part of the penis is coiled within the distal sac, and the distal part of the penis is relatively short. In light of the distinctive characteristics that distinguish this new species, we have classified it within the genus *Plagiostomum* (Platyhelminthes: Prolecithophora: Plagiostomidae). The phylogenetic tree constructed based on the concatenated datasets of 18S rDNA and 28S rDNA revealed that *P. aestuarium* is closely related to other *Plagiostomum* species. Furthermore, this study provides a comprehensive account of the distinctive reproductive biology of *P. aestuarium* and, for the first time, elucidates the function of the penis sheath structure during hypodermic insemination. This new finding could potentially serve as a new classification criterion for species within the family Plagiostomidae.

Key Words

Flatworm, mating pattern, penis sheath, phylogenetic analysis, taxonomy

Introduction

To date, more than 180 species of Prolecithophora Karling, 1940, have been recorded globally in five families and 32 genera, with the majority of the species classified in Plagiostomidae von Graff, 1882, and Pseudostomidae von Graff, 1904 (Tyler et al. 2006b).

Prolecithophora species are generally diminutive in size, characterized by the presence of elongated, sac-like

intestines. Their pharynx exhibits a pleated or deformable structure. The reproductive organs, including the testes and ovaries, are not encapsulated by any membranes but are instead diffusely distributed. Similarly, the vitellaria are also dispersed in a diffuse manner (Tyler et al. 2006a). The genital pore and the mouth of these flatworms may either open together or separately, and their positioning can be either in the anterior or posterior region of the organism (Grosbusch et al. 2021). Due to the scarcity of

molecular data for species within Prolecithophora, phylogenetic studies are somewhat constrained by insufficient data. Moreover, there are inconsistencies between morphological and phylogenetic classification results. Therefore, during classification, it is essential to comprehensively consider multiple morphological characters in conjunction with data on multiple genes. This integrative approach helps to avoid classification errors caused by convergent evolution (Norén and Jondelius 1999; Joffe and Kornakova 2001; Norén and Jondelius 2002).

The family Plagiostomidae is the most species-rich taxon within the order Prolecithophora (Tyler et al. 2006b). From a morphological perspective, the majority of species within Plagiostomidae are characterized by a fusiform body shape. They typically possess an anterior or ventral pharynx and one or two pairs of eyes, as well as paired testes and ovaries (Grosbusch et al. 2022). The family includes nine genera, namely *Acmostomum* Schmarda, 1859; *Auriculifera* Kulinitich, 1973; *Hydrolimax* Haldeman, 1842; *Plagiostomum* Schmidt, 1852; *Plicastoma* von Graff, 1904; *Puzostoma* Marcus, 1950; *Torgea* Jondelius, 1997; *Tuilica* Marcus, 1951; and *Vorticeros* Schmidt, 1852. Among the 114 species, only eight have been described during this century, and only *Plagiostomum robustum* A. Wang, 2024; *Plagiostomum plagae* Feng, Zhang, Tao, Sun & Wang, 2025; and *Plagiostomum nanhaiense* Feng, Zhang, Tao, Sun & Wang, 2025 have been recorded in China (Wang et al. 2024; Feng et al. 2025). Note that, following the International Code of Zoological Nomenclature (ICZN), we adopt the neuter endings of the species names (ICZN Article 31.2) corresponding to the neuter genus name (ICZN Article 30.2.4). Moreover, we clarify that the types of *Plagiostomum nanhaiense* (holotype, PLA-PL010 and paratypes, PLA-PL011–PLA-PL019) and *Plagiostomum plagae* (holotype, PLA-PL020 and paratypes, PLA-PL021–PLA-PL026) have been deposited at the Institute of Zoology, Chinese Academy of Sciences (IZCAS).

Reproductive behaviors have been proposed as a valuable and supplementary criterion for taxonomic categorization of flatworms (Nollen 1983; Vreys et al. 2002; Schärer et al. 2011; Singh et al. 2020; Wang et al. 2024). To date, research endeavors concerning the mating behavior of free-living flatworms have predominantly centered around the taxonomic groups of Tricladida, Macrostomida, and Polycladida (Yang et al. 2020; Brand et al. 2022; Singh et al. 2025). However, little attention has been devoted to exploring the reproductive behaviors, as well as the lifestyles and other crucial biological characteristics, of the Prolecithophora. Recent studies have shown that *Plagiostomum robustum* mates by hypodermic insemination (Wang et al. 2024). Nevertheless, a significant knowledge gap persists regarding the specific functions and roles that its diverse mating organs play during the intricate mating process.

In this study, we discovered a novel species of *Plagiostomum* (Platyhelminthes, Prolecithophora, Plagiostomidae) inhabiting the intertidal zones along the coast of South China. Through a comprehensive examination of its external

morphology, internal anatomy, and molecular phylogenetic relationships, we have ascertained the taxonomic identity of this new species. Moreover, the mating behavior of this novel species was subjected to meticulous observation and in-depth histological examination. Our study represents a pioneering effort in demonstrating the functional significance of the penis sheath structure during the mating process.

Materials and methods

Sample collection and culture

Intertidal seaweeds were rinsed, and the seawater samples were filtered using stacked plankton nets with 425 µm and 75 µm apertures (see below for details on the sampling site). The samples retained within the 75 µm mesh sieves were carefully collected and taken back to the laboratory for further analysis. Specimens were separated under a stereomicroscope (Leica EZ4, Leica Microsystems, Germany). Artificial seawater with a salinity of 25 ppt was prepared using artificial sea salt (Red Sea, USA). The specimens were placed in a six-well plate with the prepared seawater and fed daily with ground pieces of the Maricola *Paucumara falcata* Wang & Li, 2019. The artificial seawater was replaced twice a week. The temperature was controlled at 24 °C using air conditioning.

DNA extraction, amplification, sequencing, and phylogenetic analysis

DNA was extracted from three specimens that had been starved for 3 days using the E.Z.N.A. Mollusc DNA Isolation Kit (Omega, Norcross, GA, USA). Primers and the PCR protocol are listed in Table 1. The amplified DNA fragments were submitted to Beijing Prime Biotechnology Co., Ltd. for Sanger sequencing.

The 18S rDNA and 28S rDNA sequences of 42 Prolecithophora and two Tricladida (outgroup) species were downloaded from GenBank (Table 2). Multiple sequence comparisons were performed using MAFFT v7 based on the E-INS-i strategy for each of the two gene datasets (Katoh and Standley 2013). Conserved sequences were selected using GBLOCKS v.0.91b (Castresana 2000). The concatenated 18S rDNA + 28S rDNA sequences were used to construct phylogenetic trees. Phylogenetic analyses were performed using PhyloSuite (Xiang et al. 2023). ModelFinder was used to select the best-fit evolutionary model based on the Akaike Information Criterion (AIC) with the Bayes method and maximum likelihood tree (Kalyaanamoorthy et al. 2017). The maximum likelihood tree was constructed using IQ-TREE v.1.6.6 with 1,000 bootstrap replicates (Lam-Tung et al. 2015). Bayesian tree construction was performed via MrBayes v.3.2, and the Markov Chain Monte Carlo (MCMC) algorithm was run in four chains simultaneously for 2,000,000 generations, with sampling at 2,000-generation intervals and discarding 25% as burn-in (Ronquist et al. 2012).

Table 1. Primer sequences used for PCR amplification.

Gene	Primer	Sequence (5'-3')	PCR protocol	Reference
18S rDNA	HT18bF	CCTATGTAAGACCTAACCGC	94 °C (3 min), [94 °C (30 s), 54 °C (1 min 30 s), 72 °C (1 min 30 s)] *40, 72 °C (5 min).	This study
	HT18bR	ACCATCCAATCGGTAGTAGC		
28S rDNA	28SForw	TGAAGAGAGAGTTC AAKAGTACGTG	94 °C (5 min), [94 °C (30 s), 54 °C (1 min 30 s), 72 °C (1 min 30 s)] *5, [94 °C (30 s), 56 °C (1 min 30 s), 72 °C (1 min 30 s)] *35, 72 °C (5 min).	(Norén and Jondelius 2002)
	28S1940rb	TGCTACTACYACCAAGATCTG		

Table 2. Taxon names and GenBank accession numbers of 18S and 28S rDNA sequences included in phylogenetic analyses.

Taxon	18SrDNA	28SrDNA	Reference
<i>Acanthiella</i> sp.	KC869786	KC869839	(Laumer and Giribet 2014)
<i>Acmostomum dioicum</i>	AF503516	—	—
<i>Allostoma catinosum</i>	MK791294	MK791299	—
<i>Allostoma neostiliferum</i>	AF167420	—	—
<i>Allostoma pallidum</i>	AJ312265	AJ313214	(Norén and Jondelius 2002)
<i>Baicalarctia gulo</i>	AJ287483	—	(Littlewood and Olson 2001)
<i>Euxinia</i> sp.	KC869821	KC869874	(Laumer and Giribet 2014)
<i>Cylindrostoma fingsalianum</i>	AF051330	AJ313215	—
<i>Cylindrostoma gracilis</i>	AF065416	AJ313216	—
<i>Cylindrostoma</i> cf	AJ312266	AJ313223	(Norén and Jondelius 2002)
<i>Dugesia japonica</i>	D83382	DQ665966	(Katayama et al. 1996)
<i>Dugesia umbonate</i>	MT177214	MT177210	—
<i>Euxinia baltica</i>	AF167418	—	—
<i>Friedmaniella</i> cf	AJ287512	—	(Littlewood and Olson 2001)
<i>Friedmaniella karlingi</i>	AJ287513	—	(Littlewood and Olson 2001)
<i>Plagiosomum aestuarium</i> sp. nov. 1	PQ346280	PQ346283	This study
<i>Plagiosomum aestuarium</i> sp. nov. 2	PQ346281	PQ346284	This study
<i>Plagiosomum aestuarium</i> sp. nov. 3	PQ346282	PQ346285	This study
<i>Plagiosomum album</i>	AF065418	AJ313224	—
<i>Plagiosomum chromogastrum</i>	OP627003	—	(Grosbusch et al. 2022)
<i>Plagiosomum cuticulata</i>	AF065422	AY157158	(Grosbusch et al. 2022)
<i>Plagiosomum girardi</i>	OP627009	OP626912	(Grosbusch et al. 2022)
<i>Plagiosomum koreni</i>	OP627005	OP626904	(Grosbusch et al. 2022)
<i>Plagiosomum lemani</i>	AF503518	—	—
<i>Plagiosomum maculatum</i>	OP627006	OP626909	(Grosbusch et al. 2022)
<i>Plagiosomum nanhaiense</i>	PV061864	PV061865	(Feng et al. 2025)
<i>Plagiosomum ochroleucum</i>	AF065419	AJ313225	—
<i>Plagiosomum plagae</i>	PV061866	PV061867	(Feng et al. 2025)
<i>Plagiosomum robustum</i>	OR713097	OR713100	(Wang et al. 2024)
<i>Plagiosomum</i> sp. BE-2020	OP627004	OP626905	(Grosbusch et al. 2022)
<i>Plagiosomum</i> sp. MW-2019	MG882054	MG882057	—
<i>Plagiosomum</i> sp. SL-2020	MT407645	—	—
<i>Plagiosomum stellatum</i>	KC869819	KC869872	(Laumer and Giribet 2014)
<i>Plagiosomum striatum</i>	AF065420	AJ313226	—
<i>Plagiosomum vittatum</i>	AF065421	AJ313227	—
<i>Plagiosomum whitmani</i>	KC869818	KC869871	(Laumer and Giribet 2014)
<i>Protomonotresidae</i> sp.	KC869820	—	(Laumer and Giribet 2014)
<i>Protomonotresis centrophora</i>	AF167419	AJ313218	—
<i>Pseudostomum gracilis</i>	AF065423	—	—
<i>Pseudostomum klostermanni</i>	AF065424	AJ313219	—
<i>Pseudostomum quadrioculatum</i>	AF065425	—	—
<i>Reisingeria hexaoculata</i>	AF065426	AJ313220	—
<i>Scleraulophorus cephalatus</i>	AF167423	AJ313221	—
<i>Torgea phukettensis</i>	AF503517	—	—
<i>Ulianinia mollissima</i>	AF065427	AJ313222	—
<i>Vorticeros auriculatum</i>	AJ312267	AJ313229	(Norén and Jondelius 2002)
<i>Vorticeros ijimai</i>	D85094	—	(Katayama et al. 1996)

Specimen preparation for histology

The tissue preparation was performed according to the method of Wang et al. (2024). Flatworms that had been starved for 3 days were fixed with modified Bouin’s fixative (37% formaldehyde solution 15 ml, acetic acid 5 ml,

saturated aqueous picric acid 80 ml) for 1 hour. Specimens were dehydrated with gradient ethanol, cleared with xylene, and then embedded in paraffin wax (SIGMA, P3683, Switzerland, melting point: 56–57 °C) for 1 hour. Specimens were serially sectioned using a rotary microtome (LEICA, RM2235, Leica Biosystems, Germany) to

obtain histological sections with a thickness of 6 μm . The modified Cason's Mallory–Heidenhain stain was used for staining (Yang et al. 2020), and the slides were sealed with neutral gum (Maclin, Shanghai, China). Flatworm morphology was observed under a compound microscope (Nikon, Ni-U, Japan). Images were taken, and morphological data were measured using a digital microscope camera (Nikon, DS-Ri2, Japan) with professional camera software (Nikon, NIS-ELEMENTS D, Japan). The reconstructions of specimens were drawn using Adobe Photoshop 2024 (Adobe, USA) based on digital micrographs.

Mating behavior and ontogeny observations

Twenty sexually mature specimens were placed into ten flat-bottomed concave slides, each with a pair of individuals (aperture 20 mm in diameter and 1 mm in depth). The mating process was recorded with a digital microscope (Nikon, Ni-U, Japan). Upon completion of mating, the flatworms were immediately segregated and cultured separately. For the histological analysis of the mating process, some individuals were taken for fixation and tissue sectioning during the mating process.

Following mating, flatworms were cultured and subjected to systematic observation. Once oviposition occurred, adult flatworms were carefully segregated from the eggs and individually cultured in six-well plates. Cocoon ontogenesis was observed and photographed daily. The hatched individuals were separately cultured in 12-well plates. Subsequently, their developmental processes and behavioral patterns were meticulously observed and recorded daily under a microscope.

Abbreviations

b: brain; **bl:** basal lamina; **cg:** cement glands; **ds:** distal sac; **e:** eye; **fg:** frontal gland; **g:** genital pore; **in:** intestine; **m:** mouth; **o:** ovary; **od:** oviduct; **ph:** pharynx; **pe:** penis; **pg:** prostatic glands; **ps:** penis sheath; **sg:** shell glands; **sv:** seminal vesicle; **t:** testis; **va:** vagina; **vi:** vitellaria.

Results

Phylogenetic analysis

In this study, the concatenated 18S rDNA and 28S rDNA dataset of 42 Prolecithophora species was used to construct phylogenetic trees, and two Tricladida species were used as outgroups (Table 2). After alignment and trimming of non-homologous regions, the lengths of the 18S rDNA and 28S rDNA were 1,712 bp and 947 bp, respectively. After sequence assembly, the evolutionary model was selected by ModelFinder. The optimal model for the 18S rDNA Bayesian method was GTR+F+I+G4, while the optimal model for the maximum likelihood method was GTR+F+I+R4. As for the 28S rDNA, the optimal mod-

el for the Bayesian method was GTR+F+I+G4, and for the maximum likelihood method it was GTR+F+I+R4. The phylogenetic trees constructed by the Bayesian and maximum likelihood methods had the same topology, and they were therefore combined as one (Fig. 1).

As shown in Fig. 1, Prolecithophora is divided into two clades with strong support (1.00 pp, 100% bs). The genera *Euxinia*, *Friedmaniella*, *Protomonotresis*, *Baicalarctia*, *Ulianinia*, *Scleraulophorus*, *Pseudostomum*, *Allostoma*, *Cylindrostoma*, *Reisingeria*, and *Acanthiella* form a well-supported clade (clade II), consistent with previous analyses (Feng et al. 2025). Clade I contains two species of *Vorticeros*, one species each of *Torgea* and *Acmostomum*, and 19 species of *Plagiostomum*, including *P. aestuarium*, indicating that *Plagiostomum* is not monophyletic. This finding aligns with prior studies (Norén and Jondelius 1999; Wang et al. 2024; Feng et al. 2025). The three *P. aestuarium* individuals from this study formed a single branch with strong support (1.00 pp, 100% bs). Notably, ((*P. aestuarium* + *Plagiostomum* sp. SL-2020) + (*P. plagae* + *P. nanhaiense*)) and the clade comprising *Vorticeros* species ((*V. auriculatum* + *V. ijimai*) + *P. vittatum*) are sister groups with strong support (1.00 pp, 100% bs).

Systematic account

Order Prolecithophora Karling, 1940
Family Plagiostomidae von Graff, 1882
Genus *Plagiostomum* Schmidt, 1852

***Plagiostomum aestuarium* Wang & A. Wang, sp. nov.**

<https://zoobank.org/3004B0EF-53F0-48B1-BC2C-FA0FCAA588E6>

Material examined. *Holotype:* PLA-PI030, sagittal sections on two slides. *Paratypes:* PLA-PI031, sagittal sections on three slides; PLA-PI032, sagittal sections on three slides; PLA-PI033, transverse sections on six slides; PLA-PI034, horizontal sections on three slides. The type specimens were deposited in IZCAS (Institute of Zoology, Chinese Academy of Sciences).

Specimen habitat. All specimens were collected by Si-Qi Wang from the intertidal zone in Huidong County, Huizhou City, Guangdong Province, China, 22.72038°N, 114.95644°E, 30 March 2024 (Fig. 2). The specimens were collected from *Cladophora* algae. The water temperature was 24.4 °C, salinity was 25.9‰, and pH was 8.14.

Etymology. The Latin word *aestuarium* means “estuary,” and the habitat of the new species is located in an intertidal estuary.

Diagnosis. *Plagiostomum aestuarium* is distinguished by the following characters: a blunt anterior end with tentacle-like structure; a dark-brown patch covering the anterior end; a pair of black eyespots; a pair of testes and a pair of ovaries are separated, the ovaries are located anterior to the testes; the vitellaria are separated at the anterior end, merged at the dorsal part of the intestine, and separated again at the posterior end on both sides of the intestine; the penis is encased in a well-developed penis sheath; the proximal part

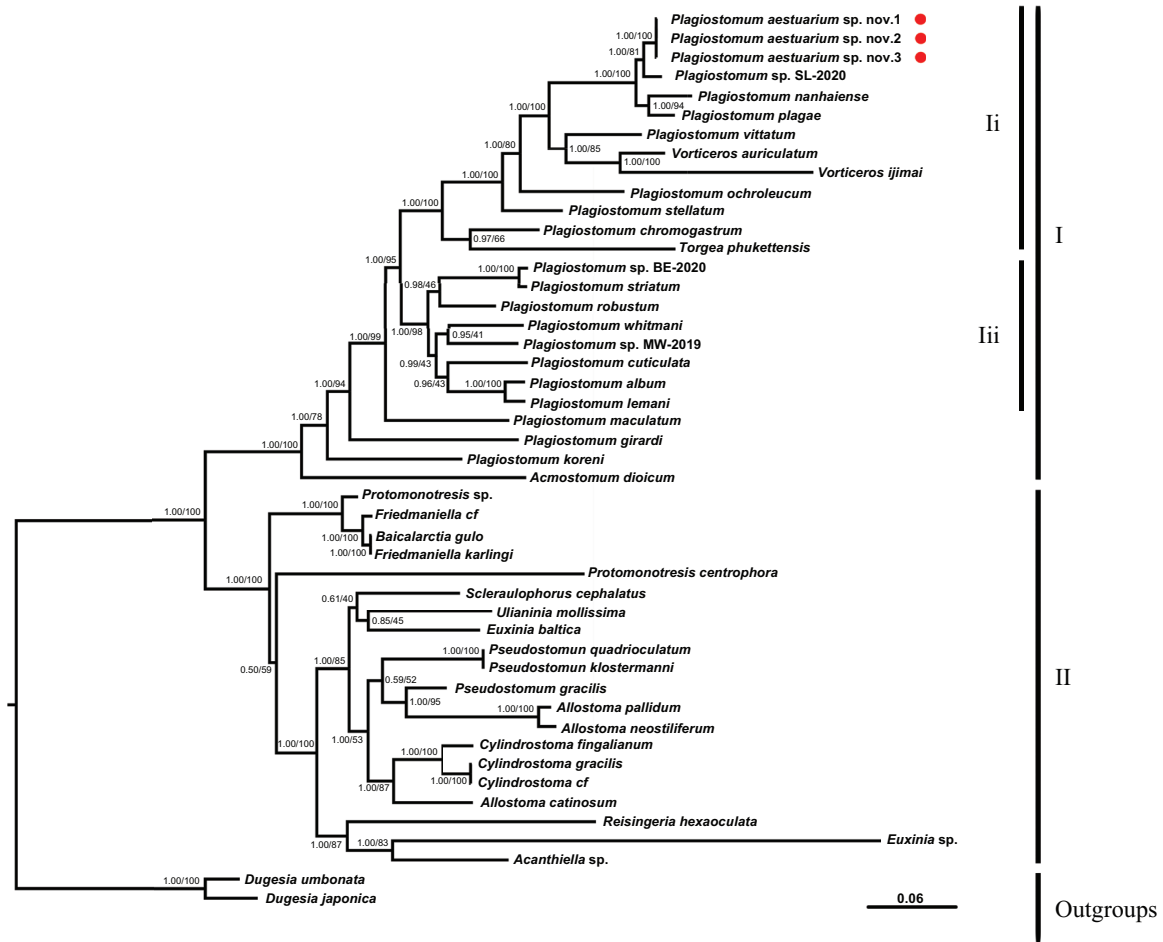


Figure 1. Phylogenetic tree based on concatenated 18S rDNA and 28S rDNA datasets (red circle: this study). Node values represent branch support: posterior probability (pp) from MrBayes and bootstrap support (bs) from IQ-TREE.

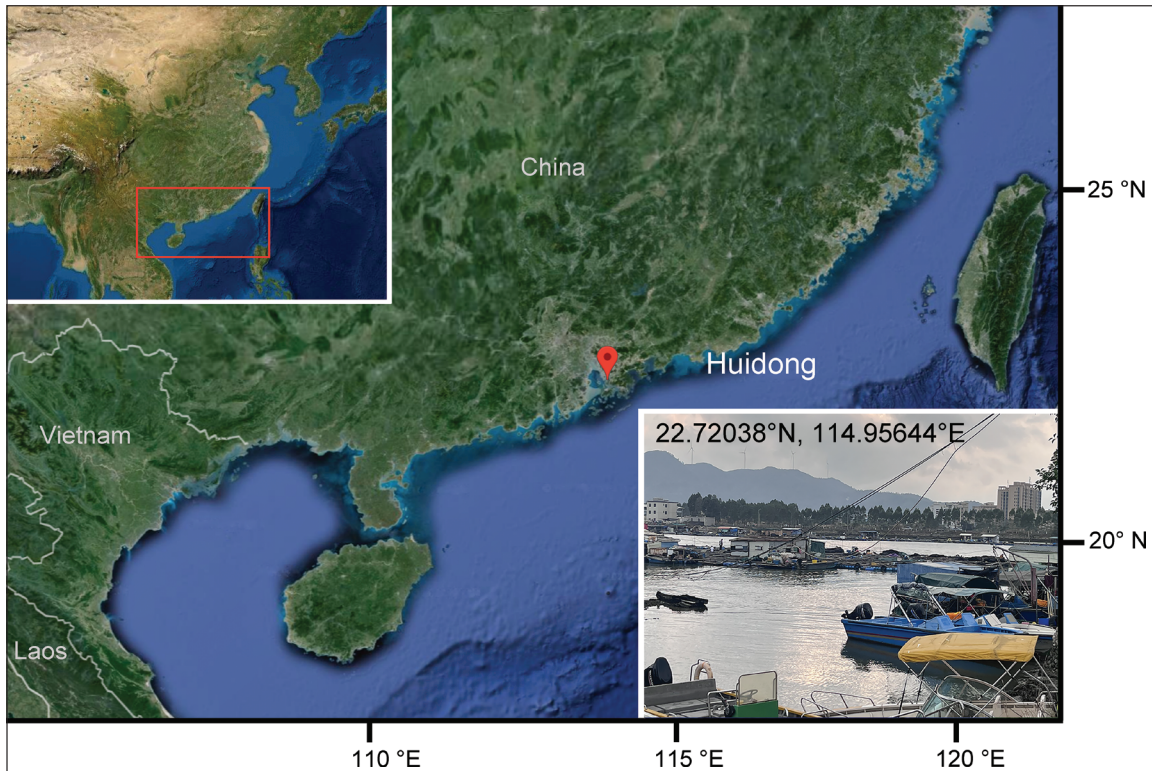


Figure 2. Habitat of *Plagiostomum aestuarium* sp. nov. (The map modified from Liu et al. 2024).

of the penis is curling up in coiling form within the distal sac, the distal part of penis is relatively short.

Description. The length of the new species is 2.05 ± 0.62 mm (mean \pm SD, $n = 9$, the same as below), and the middle body is cylindrical in cross section, 0.41 ± 0.08 mm in width (Fig. 3A). The anterior end of the body is curved and has a slight tentacle-like structure. A triangular dark-brown patch is present at the anterior end (Fig. 3A, B). A pair of black eyespots is laterally symmetrical and is located at the edge of the dark-brown patch (Figs 3B, 4B, 7E). The pharynx is about 1/3 of the body width and 1/7 of the body length, located behind the dark brown patch. (Fig. 3A, B). The ovary of the new species is located in the middle 2/5 of the body and on both sides of the body (Fig. 3A, D). The caudal end is conical (Fig. 3C, E), and five to seven clearly observable long ellipsoidal cement glands with fine tubes converge at the genital pore (Fig. 3C). The penis is attached at the posterior end of the seminal vesicle (Fig. 3E). The genital pore opens at the 1/10 near the posterior end (Fig. 3A, C, E).

The surface of the body is richly ciliated, with cilia 2/3 as long as the thickness of the epidermis (Fig. 4B-G). The basal lamina of the ventral epidermis is thick, with secretory gland cells (Fig. 4A). The anterior end has two types of frontal gland cells; the ones that are stained red by histological

staining (fig-2) are distributed within the sub-anterior epidermis, and the ones that are stained mauve-colored by the histological staining (fig-1) are filled in between the fig-2 and the brain. Both types of glands have a dense glandular duct leading to the anterior epidermis at the ventral side (Fig. 4A, F). The brain is located inferior to the eyespots and anterior to the pharynx (Fig. 4A, F). The muscular pharynx opens ventrally in the anterior region and connects to a long sac-like intestine surrounded by abundant pharynx gland cells, and the epidermis of the pharynx cavity is covered by cilia (Fig. 4A, B). The male copulatory organ is located caudally, occupying about 1/4 of the body length, and opens jointly with the female genital pore into the common genital cavity (Fig. 4A, C). The genital pore is surrounded by the dark-red stained shell glands (Fig. 4A, C, E, G).

Female reproductive organs consist of vitellaria, ovaries, oviducts, a female genital pore, shell glands, and cement glands. A pair of vitellaria extend anteriorly to the pharynx, posteriorly to the male copulatory organ, and bilaterally above the ovary, taking up 4/5 of the body length. The left and right vitellaria anterior to the ovary are separated, join at the back of the intestine, and are distributed on the two sides of the intestine behind the ovary (Figs 4A, 5A, C, E). The paired ovaries are located in the middle of the body on both sides of the intestine,

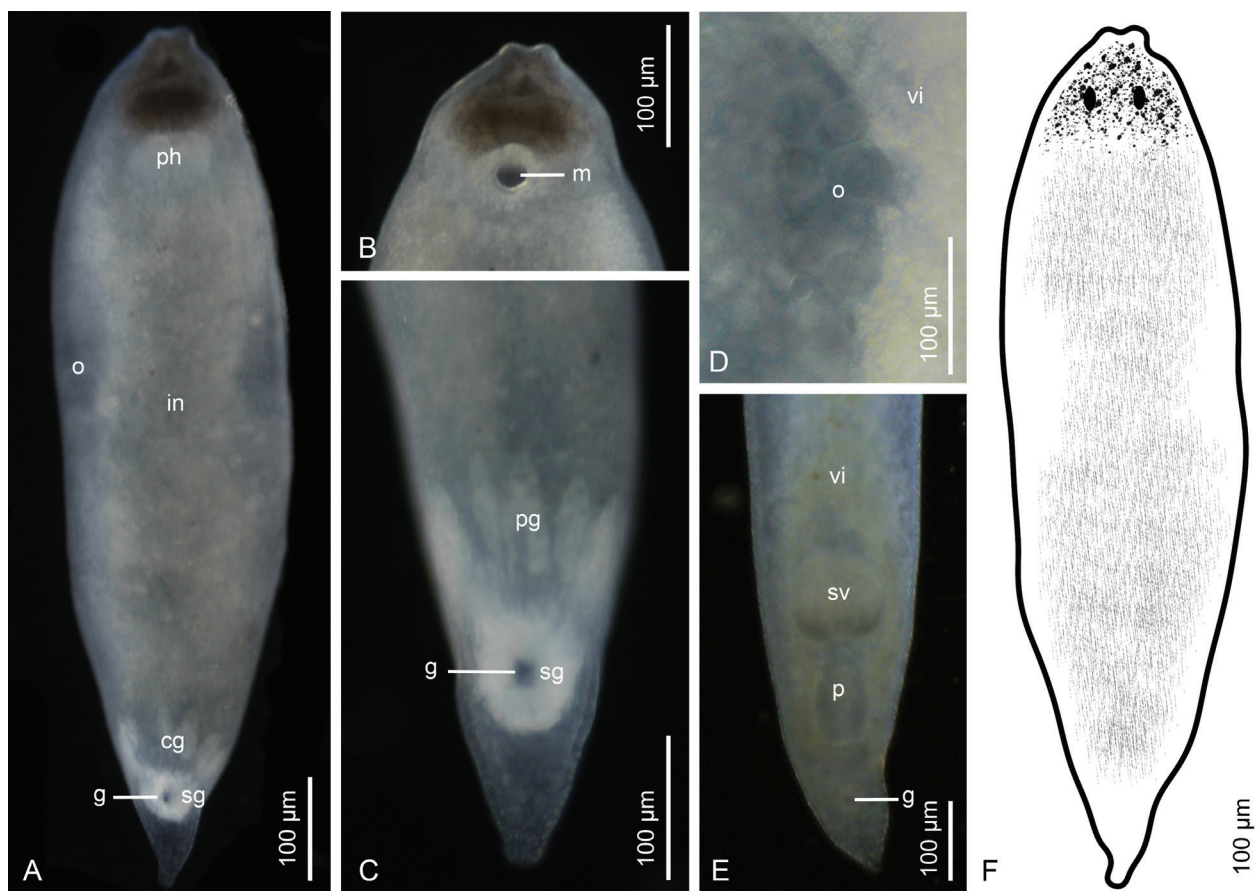


Figure 3. *Plagiostomum aestuarium* sp. nov. **A.** Living specimen, ventral view; **B.** Anterior end of a living specimen, ventral view, showing the mouth opening, a dark brown patch, and a tentacle-like structure; **C.** Posterior end of a living specimen, ventral view, showing the genital pore, shell glands surrounding the genital pore, and 5–8 long foliated cement glands; **D.** Ovaries and vitelline glands; **E.** Posterior end of a living specimen, dorsal view, showing the seminal vesicle and penis; **F.** Pigment patterns in dorsal view.

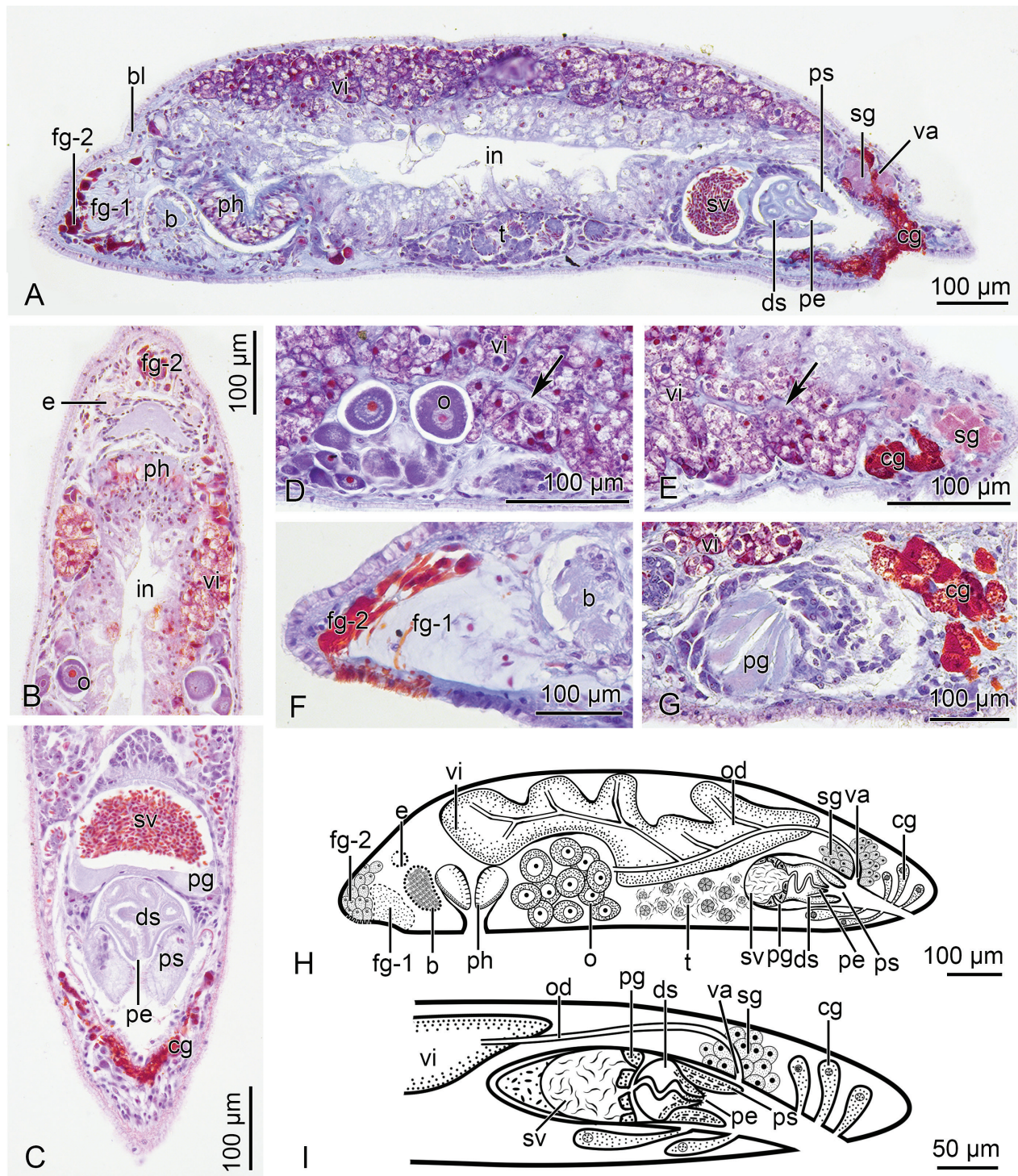


Figure 4. Sagittal and horizontal specimen and sagittal reconstruction of *Plagiostomum aestuarium* sp. nov. **A.** Holotype, PLA-P1030, sagittal section through whole specimen; **B.** Paratype, PLA-P1034, horizontal section of the anterior end; **C.** Paratype, PLA-P1034, horizontal section of the posterior end; **D.** Holotype, PLA-P1030, sagittal section showing ovaries and oviduct (arrow points); **E.** Holotype, PLA-P1030, sagittal section showing oviduct, purple shell glands, and orange-red cement glands; **F.** Holotype, PLA-P1030, sagittal section of the anterior end showing two kinds of frontal glands; **G.** Holotype, PLA-P1030, sagittal section of prostatic glands; **H.** Sagittal reconstruction of the holotype; **I.** Sagittal reconstruction of the copulatory apparatus.

proximal to the ventral side of the vitellaria, without obvious enveloping membranes (Figs 4D, E, 5A). The oviducts, about 8 μm in diameter, consist of only a layer of connective tissue and stretch from the posterior end of the ovary (Fig. 4D, E, as indicated by the arrow). Branches

of vitelline ducts converge into the oviducts (Fig. 4D, E) and then connect the egg-forming cavity. The egg-forming cavity is surrounded by abundant purple-stained shell glands. The vagina opens dorsally in the middle part of the common genital cavity (Figs 4A, D, E, 5F).

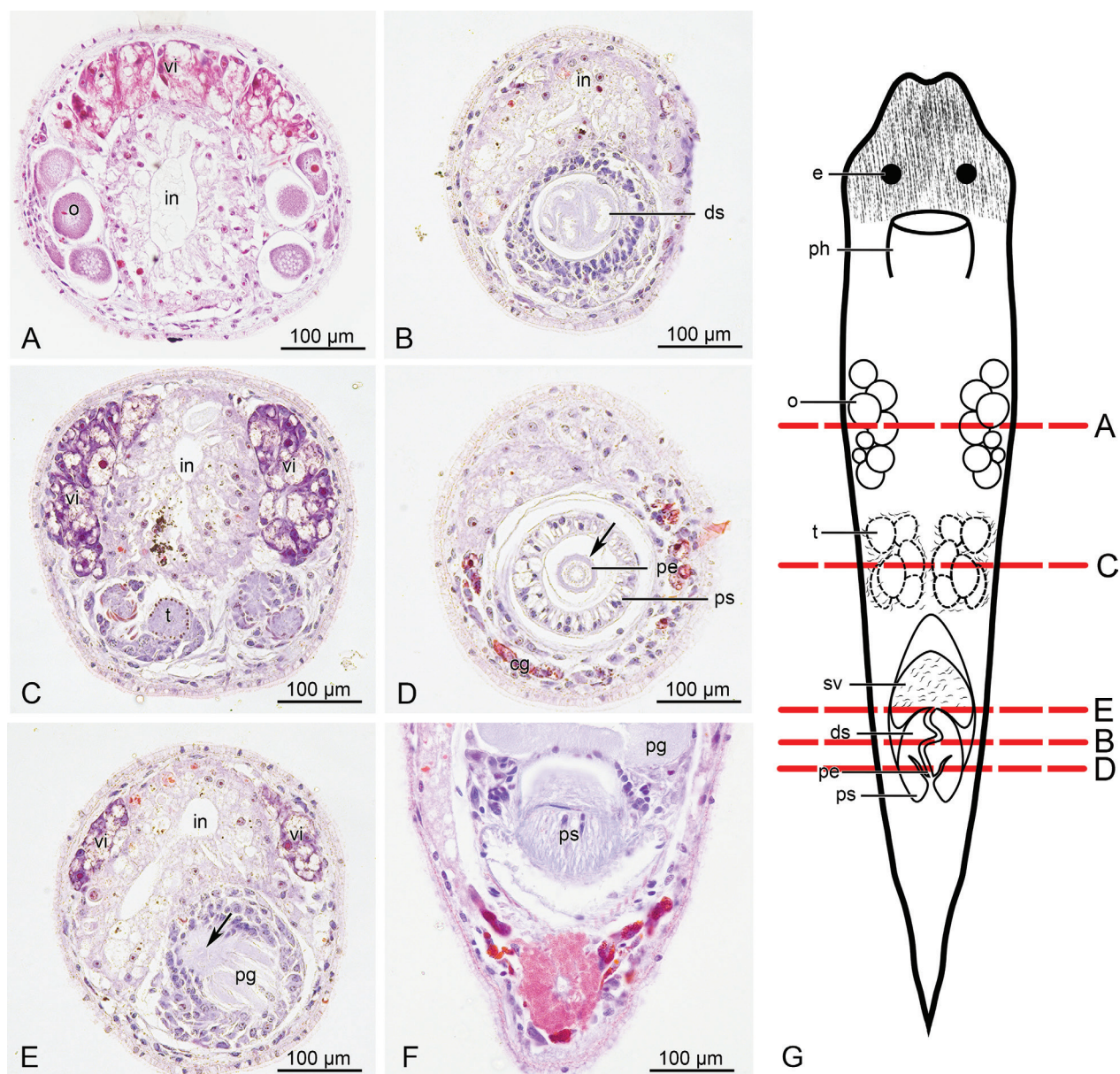


Figure 5. Transverse and horizontal sections of *Plagiostomum aestuarium* sp. nov. **A.** Paratype, PLA-PI033, transverse section of ovary, intestine, and dorsal vitellaria of the intestine; **B.** Paratype, PLA-PI033, transverse section of distal sac; **C.** Paratype, PLA-PI033, transverse section of testis, vitellaria, and intestine; **D.** Paratype, PLA-PI033, transverse section of penis and penis sheath, showing papilla-like structure (arrow); **E.** Paratype, PLA-PI033, transverse section of orifice of ejaculation (arrow); **F.** Paratype, PLA-PI034, horizontal section of posterior end, showing the shell glands and cement glands. **G.** Schematic drawing showing cutting levels of transverse sections.

Male reproductive organs consist of testis, seminal vesicle, prostatic glands, penis, distal sac, and penis sheath. The paired testes, about 1/5 of the body length, are located posterior to the ovaries and ventral to the intestine (Figs 4A, 5C). The purple-red spindle-shaped spermatozoa are present between the spermatogonia (Fig. 4A). The hemispherical seminal vesicle is located directly behind the posterior end of the testes, with no vas deferens observed (Fig. 4A, C). Several striated prostatic glands are attached to the posterior wall of the seminal vesicle, encasing the spermatogonia, and there is no separate prostatic membrane (Figs 4A, C, G, 5E). The distal sac is attached posteriorly to the seminal vesicle, a

tubular structure with a diameter of 10 μm, and shows no sperm storage during non-mating period (Figs 4A, C, 5B). The penis sheath is attached to the seminal vesicle. From outer to inner, the penis sheath consists of the outer ring muscle, radial muscle, and sleeve-shaped inner ring muscle that surrounds the penis (Figs 4A, C, 5D). The penis musculature, which terminates in a papilla-like structure, is located in the common genital cavity and is encased in the penis sheath. The penis sheath is “w”-shaped in the sagittal section and concentric in the transverse section (Figs 4A, C, 5D). The seminal vesicle, distal sac, penis, and penis sheath are encased in a layer of epithelial cells that can move together. The common genital cavity opens

on the ventral side of the caudal end and is surrounded by abundant cement glands that converge posteriorly towards the common genital pore (Fig. 4A, C, F).

Reproductive biology and individual development

Unique hypodermic insemination method

Two mating modes were observed, namely unidirectional mating and bidirectional mating, and the mating duration was about 5 minutes. Before mating, two sexually mature individuals approached each other several times, a process that took around 1 min. *Plagiostomum aestuarium* of similar size usually have a greater chance of mating. After identifying the mating partner, one of the flatworms extended its penis and the relevant organs (Fig. 6A). The extended structure is about 1/2 of the body length and includes the

prostatic glands, seminal vesicle, penis sheath, and penis. At the pre-mating phase, the muscular penis sheath sucked on the epidermis of another individual, causing the epidermis and basement membrane to protrude. Immediately after this, the penis stabbed its mating partner subcutaneously, usually in the middle part of the body, and transferred ejaculate (Fig. 6B). Via the ejaculatory ducts, the spermatozoa were injected into the subcutaneous tissue of another individual (Fig. 6E–I). Upon completion of ejaculation, the penis sheath released the epidermis of the other individual, the penis retracted into the penis sheath, and the entire copulatory organ retracted back into the body.

If only unidirectional mating occurs, mating ends with a unilateral ejaculation, and if bidirectional mating occurs, ejaculation occurs sequentially in both directions. Remarkably, we found a clear difference between bidirectional and unidirectional mating behavior. In bidirectional mating, the two individuals do not mate at the same time. One minute after one individual’s ejaculation, the other

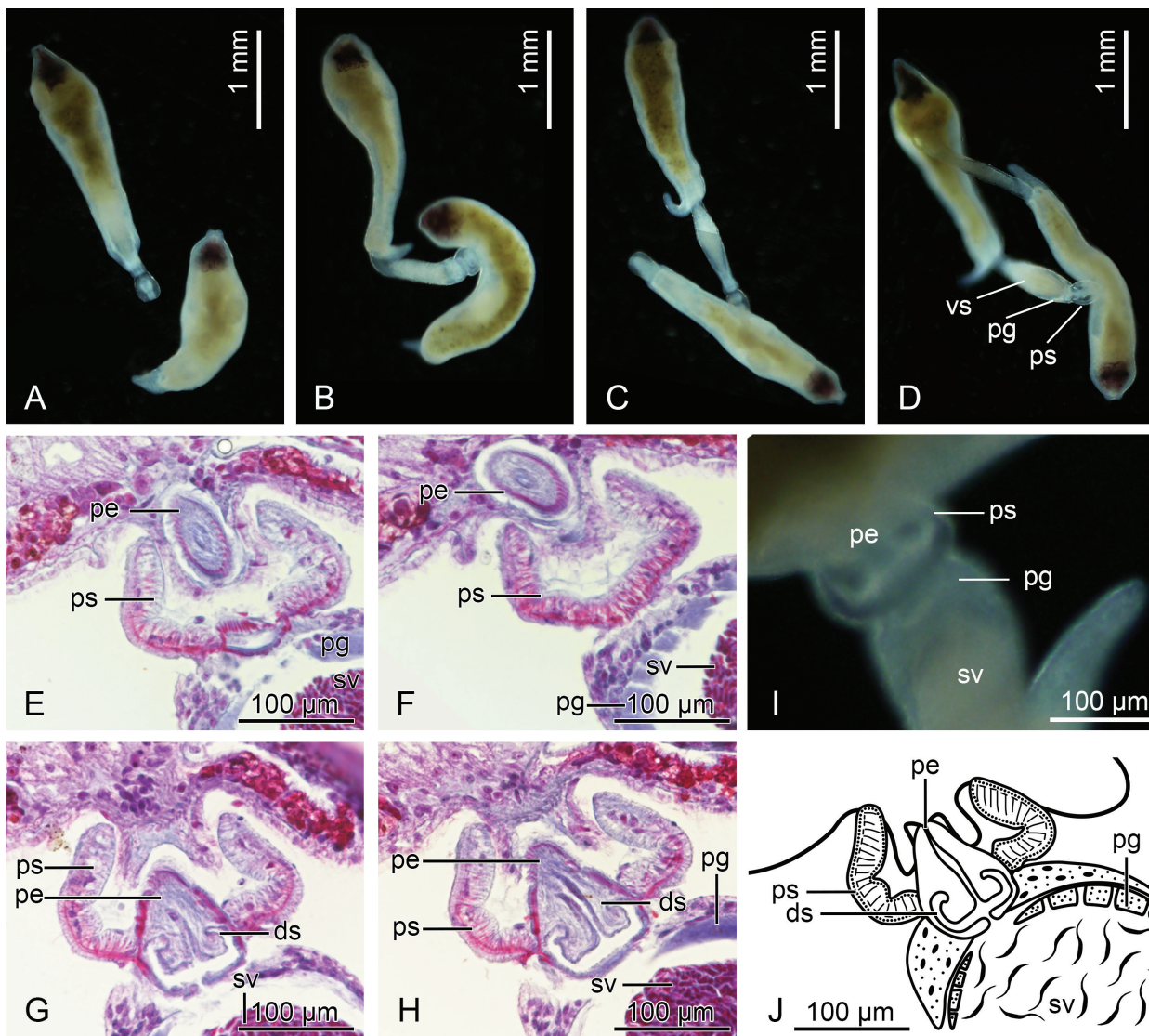


Figure 6. Mating behavior and histological analysis of *Plagiostomum aestuarium* sp. nov. **A–D.** Hypodermic insemination process (consecutive records of the same pair of samples); **E–H.** Horizontal section during mating (showing the penis part of the sperm donor); **I.** Penis inserted into each partner’s subcutaneous tissue; **J.** Reconstruction of reproductive organs during mating.



Figure 7. Oviposition, embryo development, and postembryonic development of *Plagiostomum aestuarium* sp. nov. **A–D.** Spawning behavior; **C.** late embryonic development; **D.** Flatworms hatch; **E.** Developmental age (d) and morphological changes of flatworm.

individual reached and extended its penis ($n = 13$ pairs) (Fig. 6C). Its penis sheath then sucked the partner, and its penis pierced the partner's subcutaneous tissue. Subsequently, both individuals used the penis sheath to anchor each other, followed by a stable bidirectional mating (Fig. 6D). In contrast, during unidirectional mating, the sperm recipient struggled violently, dragged the sperm donor, and swam rapidly. Towards the end of the mating, the flatworms gradually slowed down; one side retracted its penis first, followed by the retraction of another individual around 10 seconds later. Then the two flatworms swam away from each other. Among the 20 pairs of flatworms, 13 pairs showed bidirectional mating, five pairs showed unidirectional mating, and the other two did not show any mating behavior within 1 hour of observation.

Cocoon-laying behavior

White cocoons appeared in the body 1 day after mating and became yellowish in the later stages of development; the cocoon-laying cycle was 8.43 ± 4.16 days ($n = 10$, same below), 7.56 ± 3.39 cocoons were laid in one cycle, and 3.36 ± 1.21 flatworms were hatched from each cocoon. *Plagiostomum aestuarium* often lays cocoons on seaweeds.

The flatworms stopped moving before cocoon production and stayed on the seaweed or at the bottom of the container. Then, their bodies curled up and performed a circular peristaltic contraction from head to tail, pushing the cocoon toward the genital opening (Fig. 7A, B). The flatworms secreted mucus, which solidified in water to form the stalk. After the formation of the stalk, the flatworm moved forward, and the cocoon was laid at the bottom of the vessel. Cocoons were light yellow and fuzzy upon spawning and changed to orange-yellow in 1 hour.

Hatching

At 2.56 ± 1.34 days ($n = 83$, same below) of development, a distinct embryo was observed, eyespots occurred, the body of the flatworm was transparent, and the flatworm wriggled inside the cocoon shell (Fig. 7C). The cocoon ruptured after 5.45 ± 2.21 days of development, and the hatchling swam out of the shell (Fig. 7D). One cocoon hatched 3.36 ± 1.54 individuals. The flatworms hatched in a teardrop shape, with a white body and an unpigmented head, with conspicuous eyespots on the anterior part of the body and a tan substance in the intestine. Vitellaria appeared at 5 days post-hatching. At about 10 days,

brown pigment appeared between the eyespots, gradually deepening to form the typical dark-brown patch. Sexual maturity occurred at about day 25, with the appearance of a distinct ovary and penis, and mating behavior could occur. The survival rate (defined as the number of individuals surviving and developing into adults/total number of flatworms) was 25.78% (n = 256) (Fig. 7E).

Discussion

Taxonomic status

Within the genus *Plagiostomum*, the pharynx-to-body ratio and the relative positions of the testes and ovaries, as well as the structural characteristics of the male copulatory organs, serve as important bases for taxonomic identification. In species of the genus *Plagiostomum*, the testes and ovaries are diffusely distributed, lacking a surrounding membrane. The relative positions of these reproductive organs can be categorized into three types: (1) the ovaries are located anterior to the testes; (2) the ovaries are located posterior to the testes; and (3) the ovaries are situated superior to the testes. The distal and proximal parts of the penis vary in length. The proximal part of the penis acts as a vas deferens, extending or curling up. The distal part of the penis serves as an ejaculatory duct, facilitating insertion into the mating partner. Most *Plagiostomum* possess a penis sheath that envelops the distal part of the penis, with differences in the degree of its development. Typically, when the distal part of the penis is long, the corresponding penis sheath also tends to be elongated, and vice versa. In *Plagiostomum aestuarium* sp. nov., the pharynx is small in volume and opens in a downward direction, the ovary is situated anterior to the testis, the proximal part of the penis coils up within the distal sac, while the distal part of the penis is short and is surrounded by a strong penis sheath. The prostatic glands are located internally to the seminal vesicle. The genital pore opens at approximately one-tenth from the posterior end.

Previous phylogenetic studies have resolved *Plagiostomum* into two major clades. Clade Iii (comprising *Plagiostomum striatum* von Graff, 1911; *P. robustum* A. Wang, 2024; *P. whitmani* von Graff, 1911; *P. cuticulata* Brandtner, 1934; *P. album* Hyman, 1938; and *P. lemani* Forel & Du Plessis, 1874) is characterized by a larger pharynx-to-body ratio (>1/4). In contrast, clade Ii (including *P. aestuarium*; *P. nanhaiense* Feng, Zhang, Tao, Sun & Wang, 2025; *P. plagae* Feng, Zhang, Tao, Sun & Wang, 2025; *P. vittatum* Frey & Leuckart, 1847; *Vorticeros auriculatum* Müller, 1784; *V. ijimai* Tozawa, 1918; *P. ochroleucum* von Graff, 1882; *P. stellatum* von Graff, 1911; *P. chromogastrum* von Graff, 1890; and *Torgea phukettensis* Norén & Jondelius, 2004) exhibits a smaller pharynx-to-body ratio (<1/4) (Wang et al. 2024). As for *P. aestuarium*, it has a pharynx about one-third of the body width and one-seventh of the body length, which is consistent with the results of Wang et al. (2024). Among these

Plagiostomum, *P. vittatum* and *P. stellatum* have different relative positions of the reproductive organs (von Graff 1911), compared to *P. aestuarium*. *P. ochroleucum* has an external prostatic gland relative to the seminal vesicle (von Graff 1882), which can be distinguished from the internal prostatic gland of *P. aestuarium*. The proximal part of the penis in *P. chromogastrum* is extended (Westblad 1956), while in *P. aestuarium* it is coiled up within the distal sac. As for *P. plagae* and *P. nanhaiense*, molecular phylogenetic analysis showed that they are closely related to the new species. *P. plagae* has two dorsal stripes, *P. nanhaiense* has three dorsal stripes, while *P. aestuarium* has a patch covering the anterior end. Moreover, the distal part of the penis in these two species is much shorter than that of *P. aestuarium* (Feng et al. 2025).

Apart from the species in clade Ii, there are also other *Plagiostomum* species without molecular data that have a small pharynx-to-body ratio, including *Plagiostomum abboti* Karling, 1962; *P. falklandicum* Westblad, 1952; *P. girardi* Schmidt, 1857; *P. hedgpethi* Weiss, 1909; *P. koreni* Jensen, 1878; *P. morgani* von Graff, 1911; and *P. nucleipharyngeum* Karling & Jondelius, 1995. The prostatic glands of *P. abboti* and *P. falklandicum* are located externally to the seminal vesicle (Karling 1962; Karling and Jondelius 1995), which distinguishes them from *P. aestuarium*. In *P. hedgpethi*, *P. koreni*, and *P. girardi*, the ovaries are located superior to the testes (von Graff 1882; Westblad 1956; Karling 1962). By contrast, *P. aestuarium* has ovaries located anterior to the testes. The proximal part of the penis in *P. nucleipharyngeum* is extended (Westblad 1956; Karling and Jondelius 1995), while that in *P. aestuarium* is coiled up within the distal sac. The 18S and 28S rDNA sequences of *P. morgani* and *P. aestuarium* showed 100% sequence identity. Although the two species have similar external appearances (both have a dark-brown patch at the anterior end), their internal morphology is markedly different, including distinct arrangements of the testes and ovaries, as well as the structure of the penis (von Graff 1911). Therefore, the sequence labeled as *P. morgani* may have been misidentified. Of course, this requires further confirmation, as no morphological data are available for the specimen corresponding to the *P. morgani* sequences.

The anterior tentacle-like structure is the primary classification criterion of *Vorticeros*. However, in the description of *Plagiostomum robustum*, an anterior tentacle-like structure was also mentioned (Wang et al. 2024). The length ratio of the anterior tentacle-like structure to the body of *Vorticeros* species typically exceeds 1/10 (Kozloff and Westervelt 2001). Conversely, in the case of *P. robustum*, this value is only 1/40 (Wang et al. 2024). In the current study, the tentacle-like structure-to-body length ratio of *P. aestuarium* is 1/60. In light of these findings, both morphological and molecular data suggest that if only the presence or absence of the anterior tentacle-like structure is considered as a major characteristic, it is not sufficient for the classification of *Vorticeros*. Notably, we found that most species within the genus *Vorticeros* have a combination of

a “long, slender penis sheath” and a “short distal part of the penis,” with the penis sheath extending far beyond the distal part of the penis in the genital cavity. In *Plagiostomum*, this type of mating organ is exclusively found in *P. nucleipharyngeum* Karling & Jondelius, 1995. However, this species lacks a tentacle-like structure (Karling and Jondelius 1995). Therefore, we propose that for the preliminary identification of *Vorticeros*, it is more advisable to take into account both of the following features: a “slender penis sheath” accompanied by a “short distal part of the penis,” along with an anterior tentacle-like structure having a tentacle-to-body length ratio greater than 1/10.

In terms of molecular phylogeny, when compared with the results of previous studies, there is an inconsistency in the topology of the clade ((*P. album* + *P. lemani*) + *P. cuticulata*) + (*Plagiostomum* sp. MW-2019 + *P. whitmani*), which is possibly caused by different selection models (Wang et al. 2024). However, MrBayes and maximum likelihood methods generated well-supported evolutionary trees with similar topology in our study. The taxon *Plagiostomum* is paraphyletic, forming a clade with *Vorticeros* and *Torgea*. Although *P. aestuarium* and *Vorticeros* are sister groups in terms of molecular phylogeny, morphological data do not support *P. aestuarium* and *Vorticeros* as a taxonomically monophyletic group.

The non-monophyletic situation of *Plagiostomum* was also repeatedly demonstrated in previous studies. In Norén and Jondelius (2002), *Plagiostomum* was also shown to be a non-monophyletic group due to the inclusion of *Vorticeros* and *Plicastoma cuticulata*. However, *Plicastoma cuticulata* has now been transferred to *Plagiostomum*. Kozloff and Westervelt (2001) proposed that *Plagiostomum* and *Vorticeros* species are similar in morphology, and the main difference is that the latter has a pair of tentacle-like structures on the head. Norén and Jondelius (1999) proposed that *Vorticeros* should be merged with *Plagiostomum*. However, due to the obvious morphological differences in the pharynx of species in the genus *Torgea* Jondelius, 1997, even if *Plagiostomum* and *Vorticeros* were merged, the problem of the non-monophyly of *Plagiostomum* would still exist. Wang et al. (2024) proposed that *Plagiostomum* should be re-divided according to the morphology of the pharynx and penis. Due to the absence of molecular data, the taxonomic status of species in *Vorticeros* other than *V. auriculatum* and *V. ijimai* could not be determined. The morphological and phylogenetic findings of this study support the conclusion that *P. aestuarium* belongs to *Plagiostomum*, while the problem of Plagiostomidae species classification can only be resolved when wider and deeper molecular and morphological data become available.

Penis sheath and its function

Copulatory organs with different morphological characteristics often correspond to different mating forms. In species of the genus *Macrostomum* Schmidt, 1848, both

hypodermic insemination and reciprocal copulation have been observed (Brand et al. 2022), each corresponding to distinct types of male intromittent organs. *Macrostomum* species with sharp distal stylet tips usually mate through subcutaneous injection, with the stylet instantly piercing the skin tissue of another individual (Ramm et al. 2015). In contrast, *Macrostomum* species with obtuse distal stylet tips typically mate by inserting the stylet into the female genital pore (Schärer et al. 2004; Vizoso et al. 2010; Vellnow et al. 2018).

To adapt to specialized mating patterns, flatworms often evolve reproductive organs with unique structures. The penis stylet of *Gieysztoria knipovici* Zhang, 2017, and the muscular parenchymal organ of *Paucumara falcata* Wang & Li, 2019, both function to fix the sperm recipient during mating (Zhang et al. 2017; Yang et al. 2020).

The penis sheath structures have been found in many species of Prolecithophora. Notably, all species within *Plagiostomum* possess this structure, yet its function has not been clearly examined so far. von Graff (1882) once proposed a nested model, in which the penis sheath is a structure formed by the inward folding of the penis. According to this model, the structure expands during mating, and then the penis is pushed out for ejaculation. By observing the histological sections of *P. aestuarium* during the mating process, we found that the mating behavior of *P. aestuarium* did not fit the hypothesis of the nested model. During mating, the penis sheath did not expand but attached to the epidermis of the partner and served as a fixation point to assist the penis in ejaculation.

The penis of *P. aestuarium* is muscular and has a blunt, round end, which does not appear suitable for the injection mating method that requires rapid piercing of the partner's skin. However, the structure of the penis sheath is sucker-shaped, which can compensate for the limitations of the blunt and round penis. During the mating process, the penis sheath first anchored itself to the epidermis of the partner and then extended the penis to pierce the epidermis for ejaculation. This suggests that the combination of the penis sheath and the papilla-like structure on the penis is adapted to the hypodermic insemination type of mating. It is worth noting that this mating organ differs from the traditional view that typical hypodermic insemination relies on stylets. Interestingly, similar mating mechanisms have been reported in other taxa. For instance, in *Macrostomorpha* Doe, 1986, *Psammomacrostomum* sp. 1 possesses a muscular cirrus, a male genital structure lacking a hardened stylet, and performs subcutaneous sperm injection (Janssen et al. 2015). In Acoela Uljanin, 1870, *Arehaphanostoma agile* Jensen, 1878, and *Pseudaphanostoma psammophilum* Dörjes, 1968, also achieve subcutaneous insemination using a muscular cirrus (Apelt 1969). The penis sheath of *P. aestuarium* and the muscular cirrus of these aforementioned species exhibit functional convergence: both achieve penetration of the body wall through non-hardened muscular structures. These findings suggest that hypodermic insemination may be achieved through diverse types of mating organs, rather than relying solely

on the traditional view that a hardened stylet is essential. This divergence underscores the evolutionary plasticity of mating organs in flatworms, where distinct morphological solutions can emerge to solve the same functional challenge of subcutaneous sperm transfer.

Our study provides the first detailed description of the function of the penis sheath. Due to the lack of available data, we can only speculate whether other *Plagiostomum* species may also exhibit this special mating behavior. However, this statement can only be confirmed after further in-depth research and more comprehensive data collection.

Acknowledgments

This study was supported by grants from the Special Fund for the Cultivation of Scientific and Technological Innovation of College Students in Guangdong Province (“Climbing Program” Special Funds; grant no. pdjh2023a0440), the China Undergraduate Training Program for Innovation and Entrepreneurship (grant no. S202410590071), and the Shenzhen University Innovation Development Fund (grant no. 2023282), as well as a grant from the Scientific and Technical Innovation Council of Shenzhen Government (grant no. jcyj20210324093412035) to Yu Zhang. We sincerely thank Ying Zhu from Westlake University for providing valuable comments on this manuscript and Miaomiao Xiong and Zhiwei Lin from Shenzhen University for assistance with specimen culture.

References

- Apelt G (1969) Fortpflanzungsbiologie, entwicklungszyklen und vergleichende frühentwicklung acoeler Turbellarien. *Marine Biology* 4(4): 267–325. <https://doi.org/10.1007/BF00350360>
- Brand JN, Harmon LJ, Schärer L (2022) Mating behavior and reproductive morphology predict macroevolution of sex allocation in hermaphroditic flatworms. *BMC Biology* 20(1): 35. <https://doi.org/10.1186/s12915-022-01234-1>
- Castresana J (2000) Selection of conserved blocks from multiple alignments for their use in phylogenetic analysis. *Molecular Biology and Evolution* 17(4): 540–552. <https://doi.org/10.1093/oxfordjournals.molbev.a026334>
- Feng L, Zhang S, Tao M, Sun T, Wang A (2025) Two new species of *Plagiostomum* (Prolecithophora, Plagiostomidae) from China with its morphology, phylogeny, and reproductive strategy. *Frontiers in Marine Science* 12: 1520497. <https://doi.org/10.3389/fmars.2025.1520497>
- Grosbusch AL, Bertemes P, Egger B (2021) The serotonergic nervous system of prolecithophorans shows a closer similarity to fecampiids than to triclad (Platyhelminthes). *Journal of Morphology* 282(4): 574–587. <https://doi.org/10.1002/jmor.21332>
- Grosbusch AL, Bertemes P, Kauffmann B, Gotsis C, Egger B (2022) Do not lose your head over the unequal regeneration capacity in Prolecithophoran flatworms. *Biology* 11(11): 1588. <https://doi.org/10.3390/biology11111588>
- Janssen T, Vizoso DB, Schulte G, Littlewood DTJ, Waeschenbach A, Schärer L (2015) The first multi-gene phylogeny of the Macrostromorpha sheds light on the evolution of sexual and asexual reproduction in basal Platyhelminthes. *Molecular Phylogenetics and Evolution* 92: 82–107. <https://doi.org/10.1016/j.ympev.2015.06.004>
- Joffe BI, Kornakova EE (2001) Flatworm phylogeneticist: Between molecular hammer and morphological anvil. In: *Interrelationships of the Platyhelminthes*. CRC Press, 279–291. <https://doi.org/10.1201/9781482268218>
- Kalyaanamoorthy S, Minh BQ, Wong TKF, Von Haeseler A, Jermini LS (2017) ModelFinder: Fast model selection for accurate phylogenetic estimates. *Nature Methods* 14(6): 587–589. <https://doi.org/10.1038/nmeth.4285>
- Karling T (1962) Marine Turbellaria from the Pacific coast of North America. I. Plagiostomidae. *Arkiv för Zoologi* 15: 125–129.
- Karling T, Jondelius U (1995) An East-Pacific species of *Multipeniata* Nasonov and three Antarctic *Plagiostomum* species (Platyhelminthes, Prolecithophora). *Meiofauna Marina* 10: 150–152.
- Katayama T, Nishioka M, Yamamoto M (1996) Phylogenetic relationships among turbellarian orders inferred from 18S rDNA sequences. *Zoological Science* 13(5): 747–756. <https://doi.org/10.2108/zsj.13.747>
- Katoh K, Standley DM (2013) MAFFT multiple sequence alignment software version 7: Improvements in performance and usability. *Molecular Biology and Evolution* 30(4): 772–780. <https://doi.org/10.1093/molbev/mst010>
- Kozloff EN, Westervelt CA (2001) *Vorticeros praedatorium* sp. nov. (Platyhelminthes: Prolecithophora: Plagiostomidae) from the Pacific coast of North America. *Cahiers de Biologie Marine* 42: 302–314.
- Lam-Tung N, Schmidt HA, von Haeseler A, Bui QM (2015) IQ-TREE: A fast and effective stochastic algorithm for estimating maximum-likelihood phylogenies. *Molecular Biology and Evolution* 32(1): 268–274. <https://doi.org/10.1093/molbev/msu300>
- Laumer CE, Giribet G (2014) Inclusive taxon sampling suggests a single, stepwise origin of ectolecithality in Platyhelminthes. *Biological Journal of the Linnean Society. Linnean Society of London* 111(3): 570–588. <https://doi.org/10.1111/bij.12236>
- Littlewood DTJ, Olson PD (2001) Small subunit rDNA and the Platyhelminthes: Signal, noise, conflict and compromise. In: *Interrelationships of the Platyhelminthes*. 25. CRC Press, 1–33.
- Liu H, Lin D, Wang A, Hu Z, Zhang Y (2024) Description of a new marine flatworm of *Prosthlostomum* (Platyhelminthes, Polycladida, Prosthlostomidae) from the South China Sea. *Zoosystematics and Evolution* 100(2): 437–445. <https://doi.org/10.3897/zse.100.114482>
- Nollen PM (1983) Patterns of sexual reproduction among parasitic platyhelminths. *Parasitology* 86(4): 99–120. <https://doi.org/10.1017/S0031182000050861>
- Norén M, Jondelius U (1999) Phylogeny of the Prolecithophora (Platyhelminthes) inferred from 18S rDNA sequences. *Cladistics* 15(2): 103–112. <https://doi.org/10.1111/j.1096-0031.1999.tb00252.x>
- Norén M, Jondelius U (2002) The phylogenetic position of the Prolecithophora (Rhabditophora, ‘Platyhelminthes’). *Zoologica Scripta* 31(4): 403–414. <https://doi.org/10.1046/j.1463-6409.2002.00082.x>
- Ramm SA, Schlatter A, Poirier M, Schärer L (2015) Hypodermic self-insemination as a reproductive assurance strategy. *Proceedings. Biological Sciences* 282(1811): 20150660. <https://doi.org/10.1098/rspb.2015.0660>
- Ronquist F, Teslenko M, van der Mark P, Ayres DL, Darling A, Höhna S, Larget B, Liu L, Suchard MA, Huelsenbeck JP (2012) MrBayes 3.2: Efficient bayesian phylogenetic inference and model choice across a large model space. *Systematic Biology* 61(3): 539–542. <https://doi.org/10.1093/sysbio/sys029>

- Schärer L, Joss G, Sandner P (2004) Mating behaviour of the marine turbellarian *Macrostomum* sp.: These worms suck. *Marine Biology* 145: 373–380. <https://doi.org/10.1007/s00227-004-1314-x>
- Schärer L, Littlewood DTJ, Waeschenbach A, Yoshida W, Vizoso DB (2011) Mating behavior and the evolution of sperm design. *Proceedings of the National Academy of Sciences of the United States of America* 108(4): 1490–1495. <https://doi.org/10.1073/pnas.1013892108>
- Singh P, Ballmer DN, Laubscher M, Schärer L (2020) Successful mating and hybridisation in two closely related flatworm species despite significant differences in reproductive morphology and behaviour. *Scientific Reports* 10(1): 12830. <https://doi.org/10.1038/s41598-020-69767-5>
- Singh P, Brand JN, Schärer L (2025) Evolution and co-evolution of the suck behaviour, a postcopulatory female resistance trait that manipulates received ejaculate. *BMC Biology* 23(1): 87. <https://doi.org/10.1186/s12915-025-02171-5>
- Tyler S, Schilling S, Hooge M, Bush LF (2006a) Turbellarian taxonomic database. <https://turbellaria.umaine.edu/> [April 18, 2025]
- Tyler S, Artois T, Schilling S, Hooge M, Bush LF (2006b) World list of turbellarian worms: Acoelomorpha, Catenulida, Rhabditophora. Prolecithophora. <https://www.marinespecies.org/turbellarians/aphia.php?p=taxdetails&id=2854> [April 18, 2025]
- Vellnow N, Marie-Orleach L, Zadesenets KS, Schärer L (2018) Bigger testes increase paternity in a simultaneous hermaphrodite, independently of the sperm competition level. *Journal of Evolutionary Biology* 31(2): 180–196. <https://doi.org/10.1111/jeb.13212>
- Vizoso DB, Rieger G, Schärer L (2010) Goings-on inside a worm: Functional hypotheses derived from sexual conflict thinking: Post-copulatory sexual conflicts. *Biological Journal of the Linnean Society*. *Linnean Society of London* 99(2): 370–383. <https://doi.org/10.1111/j.1095-8312.2009.01363.x>
- von Graff L (1882) *Monographie der Turbellarien I. Rhabdocoelida*. Verlag Wilhelm Engelmann 389: 6–13.
- von Graff L (1911) *Acoela, Rhabdocoela und Alloecoela des ostens der vereinigten staaten von Amerika*. *Zeitschrift für Wissenschaftliche Zoologie* 99: 321–428.
- Vreys C, Crain J, Hamilton S, Williamson S, Steffanie N (2002) Evidence for unconditional sperm transfer and sperm-dependent parthenogenesis in a hermaphroditic flatworm (*Girardia tigrina*) with fissipary. *Journal of Zoology* 257(1): 43–52. <https://doi.org/10.1017/S095283690200064X>
- Wang Y, Huang J, Zhang Y, Wang A (2024) Molecular phylogeny and ethology of the family Plagiostomidae (Platyhelminthes, Prolecithophora), with integrative description of a new species, *Plagiostomum robusta* A. Wang, sp. nov. *Frontiers in Marine Science* 11: 1332011. <https://doi.org/10.3389/fmars.2024.1332011>
- Westblad E (1956) Marine “Alloecoels” (Turbellaria) from North Atlantic and Mediterranean coasts. II. A new freshwater *Plagiostomum* species. *Arkiv för Zoologi* 9: 131–174.
- Xiang Y, Gao F, Jakovli I, Hu Y, Zhang H, Zou H, Wang T, Zhang D (2023) Using phylosuite for molecular phylogeny and tree-based analyses. *iMeta* 2(1): e87. <https://doi.org/10.1002/imt2.87>
- Yang Y, Li J, Sluys R, Li W, Li S, Wang A (2020) Unique mating behavior, and reproductive biology of a simultaneous hermaphroditic marine flatworm (Platyhelminthes, Tricladida, Maricola). *Invertebrate Biology* 139(1): e12282. <https://doi.org/10.1111/ivb.12282>
- Zhang L, Cai H, Bao S, Zhou J, Wang A (2017) A new record of turbellarian species (Rhabdocoela, Dalyelliidae) from China with morphological description and phylogenetic analysis. *Sichuan Journal of Zoology* 36: 65–74.